STARS

University of Central Florida
STARS

Faculty Bibliography 2000s

Faculty Bibliography

1-1-2006

Characteristic analysis of a refractive axicon system for optical trepanning

D. Zeng
University of Central Florida

W. P. Latham

A. Kar
University of Central Florida

Find similar works at: https://stars.library.ucf.edu/facultybib2000
University of Central Florida Libraries http://library.ucf.edu

This Article is brought to you for free and open access by the Faculty Bibliography at STARS. It has been accepted for inclusion in Faculty Bibliography 2000s by an authorized administrator of STARS. For more information, please contact STARS@ucf.edu.

Recommended Citation

Zeng, D.; Latham, W. P.; and Kar, A., "Characteristic analysis of a refractive axicon system for optical trepanning" (2006). *Faculty Bibliography 2000s*. 6752.
https://stars.library.ucf.edu/facultybib2000/6752

University of Central Florida
STARS
Showcase of Text, Archives, Research & Scholarship

Characteristic analysis of a refractive axicon system for optical trepanning

D. Zeng, MEMBER SPIE
University of Central Florida
College of Optics and Photonics
Mechanical, Materials and Aerospace Engineering Department
Center for Research and Education in Optics and Lasers
Laser-Aided Manufacturing, Materials and Micro-Processing Laboratory
Orlando, Florida 32816-2700

W. P. Latham, FELLOW SPIE
Air Force Research Laboratory
Directed Energy Directorate
3550 Aberdeen Avenue SE
Kirtland Air Force Base
New Mexico 87117-5776

A. Kar
University of Central Florida
College of Optics and Photonics
Mechanical, Materials and Aerospace Engineering Department
Center for Research and Education in Optics and Lasers
Laser-Aided Manufacturing, Materials and Micro-Processing Laboratory
Orlando, Florida 32816-2700

Abstract. An annular beam provides a new laser drilling mechanism, which we refer to as *optical trepanning*. A refractive axicon system has been designed to transform an input Gaussian laser beam into a collimated annular beam. The diffractive effects of the axicon system and a convex lens focusing the collimated annular beam have been studied using the Fresnel diffraction integral. The theoretical diffraction patterns are compared with the patterns measured with a laser-beam analyzer. The results show that the refractive axicon system can produce Gaussian-like annular beams with the capability of easily adjusting the size of the annular beam. © *2006 Society of Photo-Optical Instrumentation Engineers.* [DOI: 10.1117/1.2353119]

Subject terms: axicon; optical trepanning; annular beam; geometric optics; diffraction.

Paper 050830R received Oct. 17, 2005; revised manuscript received Feb. 28, 2006; accepted for publication Mar. 1, 2006; published online Sep. 19, 2006. This paper is a revision of a paper presented at the SPIE conference on Laser Beam Shaping VI, Aug. 2005, San Diego, California. The paper presented there appears (unrefereed) in SPIE proceedings Vol. 5876.

1 Introduction

Laser drilling is widely used in aerospace industries for drilling small-diameter cooling holes in combustion rings, turbine blades, and nozzle guide vanes.[1] The drilling process involves melting the material with a laser beam and expelling the melt with an assist gas, or vaporizing the material. Often oxygen is used as an assist gas to induce metal burning at the laser-beam–material interaction zone in order to increase the drilling speed.

Percussion drilling and trepanning are two traditional laser drilling methods. In percussion drilling, the laser beam is usually focused to the required hole diameter and one or more pulses of laser energy are supplied to the substrate.[1] Both the laser beam and the substrate remain stationary in this process. Trepanning, in contrast, involves cutting a hole by moving a small laser spot in a larger orbit, using either an optical element or an *x-y* galvo scanner. Trepanning also can be achieved by rotating the workpiece. These conventional processes are referred to as *mechanical trepanning* in this study.

An annular laser beam provides a new drilling mechanism. When an annular beam is focused on the workpiece surface, the material within the annulus is heated, melted and possibly vaporized, and removed to drill a hole. This process, which we refer to as *optical trepanning*, involves no rotating optics or any motion of the workpiece.[2]

Laser beams with annular transverse cross sections have been investigated for different types of applications such as atom trapping and guiding,[3,4] optical confinement of cold atoms,[5,6] laser machining,[7,8] and optical data storage.[9] An annular beam can be generated by a variety of methods. Conic lenses such as axicon and waxicon lenses are used most frequently to generate annular beams. Such optical elements provide flexibility in tailoring the size of the focused annular laser spot. Annular laser beams with variable inner and outer radii can be generated using an optical system consisting of axicon lenses and a convex lens.[10–14]

Axicon lenses are usually defined as optical elements that image a point into a line segment along the optical axis.[10,11] The axicon lens is a conical surface of revolution capable of blending light from a point source, which is located on the axis of revolution, by reflection or refraction or both.[15,16] A refractive axicon lens was described by Mcleod[10] in 1954. A glass cone refracts all rays at the same angle relative to the optical axis. A similar effect can be obtained using a reflecting cone.[1] Flores[15] presented a method for designing spherically symmetric gradient-index (index of refraction) axicon lenses, which produce a variety

0091-3286/2006/$22.00 © 2006 SPIE

Downloaded From: https://www.spiedigitallibrary.org/journals/Optical-Engineering on 27 Aug 2019
Terms of Use: https://www.spiedigitallibrary.org/terms-of-use

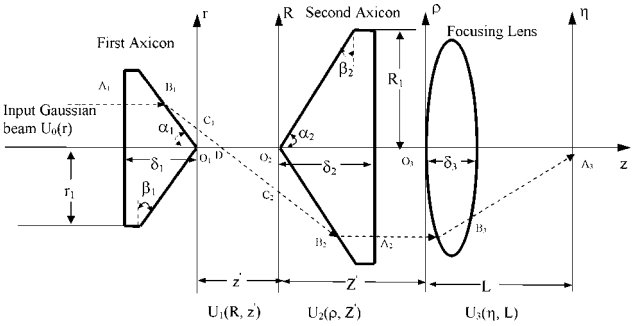

Fig. 1 Geometrical configuration of an axicon refractive system.

of different irradiance patterns along the optical axis, and with a boundary refraction index larger than or equal to the refraction index of the surrounding medium. The diffractive version of the axicon lens is rather common today.[16–19] Sochacki et al.[17] employed a ray-tracing technique together with the conservation of energy in ray bundles to design diffractive axicon lenses having the optimal phase retardation function that produces the desired on-axis irradiance. Lens axicons[20] have been proposed as an easier, cheaper, and more efficient alternative to other types of axicons. The simplest forward-type lens axicon is composed of a diverging third-order spherically aberrated lens and a perfect converging lens.

The axicons and their combinations have been used for many applications. Rioux et al.[8,9] combined an axicon lens and a convex lens to form an optical system producing an annular beam for drilling good-quality large-diameter holes using a high-power laser beam. The ring beams have also attracted increasing interest in the field of laser cooling and trapping of neutral atoms.[3] Axicons have been used to generate intense nondiffracting beams.[21–24] Studies on nondiffracting beams by Durnin et al.[23,24] drew interest to axicon optics. It has been shown that an axicon can generate a Bessel beam, a so-called nondiffracting beam, which means the irradiance pattern of the beam propagating in free space remains unchanged in the transverse plane. The central irradiance profile of such a beam can be extremely narrow, with effective diameter as small as several wavelengths, and yet possess an infinite depth of field. Such beams can be applied to imaging, metrology, dispersionless optical system design, and the production of plasma waveguides.[21–24]

We have designed an axicon refraction system for laser-beam shaping based on the diffraction theory to transform a Gaussian circular beam into an annular beam.[25] Two refractive arrangements have been developed that transform a Gaussian circular laser beam into an annular laser beam with required irradiance profiles. We also examine a certain region of the diffraction field from which the light beam evolves into an annular beam.

2 Diffraction Analysis of an Axicon Refractive System

2.1 *Fresnel Approximation of the Diffraction Field after the First Axicon Lens*

Figure 1 shows the propagation of an arbitrary ray through a refractive axicon system. The incident ray A_1B_1 intersects the optical axis at point D, and then it is collimated to the ray B_2A_2 by the second axicon lens. Here β_1 and β_2 are the base angles of the first and the second axicon lenses, respectively. The surface constraint for the axicon refractive system is $\beta_1=\beta_2$ to achieve collimation. For diffractive analysis of the beam propagation, we consider an input Gaussian electric field illuminating the flat surface of the first axicon. The amplitude of the Gaussian electric field, $U_0(r)$, can be written as follows in polar coordinates for rotationally symmetric systems:

$$U_0(r) = \sqrt{I_0}\exp\left(\frac{-r^2}{r_w^2}\right), \tag{1}$$

where r_w is the radius from the point of maximum irradiance I_0 to the point where the irradiance of the input Gaussian laser beam is I_0/e^2, and r is the radius of any point on a transverse plane.

To simplify the calculation of the optical phase function, the Gaussian beam is assumed to enter the axicon lens as a plane wave. This assumption is strictly true only if the input plane of the axicon lens coincides with the beam waist within the Rayleigh zone. As a ray travels from left (A_1B_1) to right (B_1C_1) in Fig. 1, the optical phase delay $\phi_1(r)$ introduced by the first axicon lens and the air is[26,27]

$$\phi_1(r) = kn(\delta_1 - r_1\tan\beta_1) + kn(r_1 - r)\tan\beta_1 + \frac{n_0 kr\tan\beta_1}{\cos\theta_1}, \tag{2}$$

where

$$\theta_1 = \arcsin\left(\frac{n\sin\beta_1}{n_0}\right) - \beta_1, \tag{3}$$

δ_1 is the thickness of the first axicon lens along its optical axis, r_1 is the radius of the first axicon lens, k is the wave number of the incident laser beam, and n and n_0 are the refractive indices of the axicon lens and the surrounding medium, respectively. So the transmittance function $t_1(r)$ of the first axicon lens is

$$t_1(r) = \begin{cases} \exp[i\phi_1(r)] & \text{for } r < r_1, \\ 0 & \text{for } r \geqslant r_1. \end{cases} \tag{4}$$

Neglecting the constant phase factor $\exp(ikn\delta_1)$,[28] the diffraction field $U_1(r,z)$ at a distance z' from the axicon tip O_1 along the optical axis can be written as follows in polar coordinates for rotationally symmetric systems by the Fresnel diffraction integral:[28,29]

$$U_1(R,z') = \frac{k\exp(ikz')}{iz'}\exp\left(\frac{ikR^2}{2z'}\right)\int_0^{r_1}\exp\left(\frac{-r^2}{r_w^2}\right) \times\exp\left(\frac{ikr^2}{2z'}\right)\exp\left[ikr\tan\beta_1\left(\frac{1}{\cos\theta_1} - n\right)\right] \times J_0\left(\frac{krR}{z'}\right)r\,\mathrm{d}r. \tag{5}$$

Downloaded From: https://www.spiedigitallibrary.org/journals/Optical-Engineering on 27 Aug 2019
Terms of Use: https://www.spiedigitallibrary.org/terms-of-use

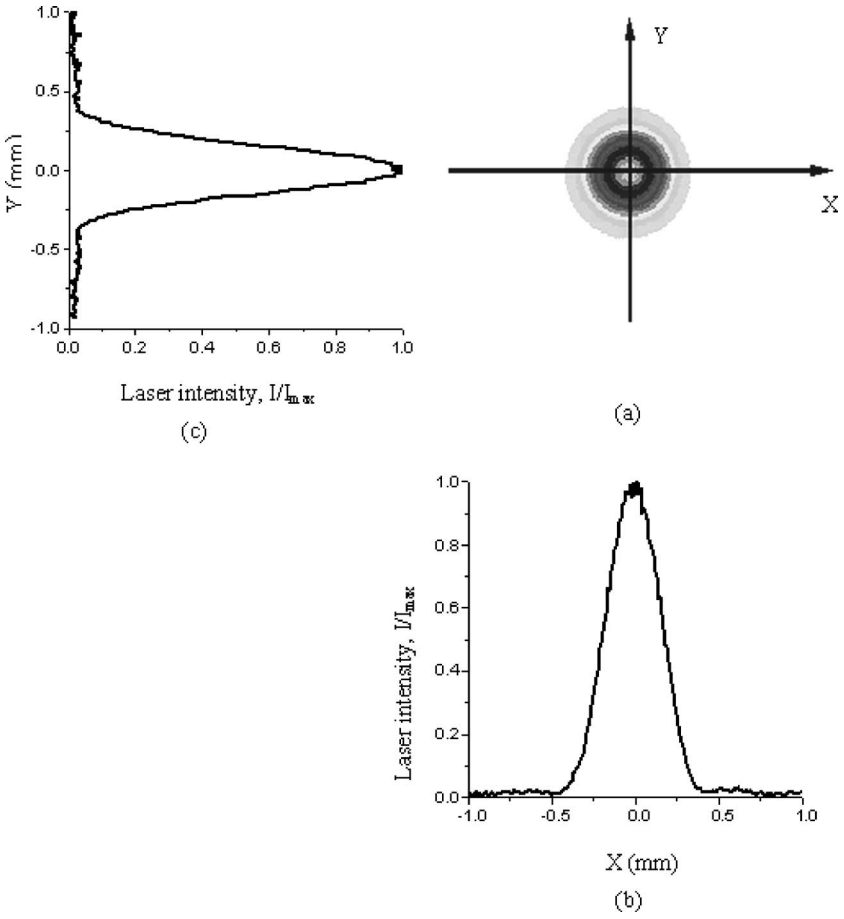

Fig. 2 Irradiance profile of an input Gaussian laser beam before the first axicon lens. (a) Transverse cross section of the annular beam profile. (b) Laser irradiance profile in the *X* direction on the transverse plane. (c) Laser irradiance profile in the *Y* direction on the transverse plane. Radius of the input Gaussian beam, r_w=0.327 mm.

2.2 *Fresnel Approximation of the Diffraction Fields after the Second Axicon Lens*

As a ray travels from left (C_2B_2) to right (B_2A_2) in Fig. 1, the optical phase delay $\phi_2(R)$ introduced by the second axicon lens and the air is[28,29]

$$\phi_2(R) = kn(\delta_2 - R_1 \tan \beta_2) + kn(R_1 - R)\tan \beta_2 + \frac{kn_0 R \tan \beta_2}{\cos \theta_2}, \tag{6}$$

where

$$\theta_2 = \arcsin\left(\frac{n \sin \beta_2}{n_0}\right) - \beta_2, \tag{7}$$

δ_2 is the thickness of the second axicon lens along its optical axis, and R_1 is the radius of the second axicon lens. So the transmittance function $t_2(R)$ of the second axicon lens is

$$t_2(R) = \begin{cases} \exp[i\phi_2(R)] & \text{for } R < R_1, \\ 0 & \text{for } R \geqslant R_1. \end{cases} \tag{8}$$

Neglecting the constant phase factor $\exp(ikn\delta_2)$,[28] the diffraction field $U_2(\rho, Z')$ at a distance Z' from the second axicon tip O_2 along the optical axis can be written as follows in polar coordinates for rotationally symmetric systems by the Fresnel diffraction integral:[28,29]

$$U_2(\rho, Z') = \frac{k \exp(ikZ')}{iZ'} \exp\left(\frac{ik\rho^2}{2Z'}\right) \int_0^{R_1} U_1(R, z') \times \exp\left(\frac{ikR^2}{2Z'}\right) \exp\left[ikR \tan \beta_2 \left(\frac{1}{\cos \theta_2} - n\right)\right] \times J_0\left(\frac{kR\rho}{Z'}\right) R \, dR. \tag{9}$$

2.3 *Fresnel Approximation of the Diffraction Fields after the Focusing Lens*

As a ray travels from left (B_2A_2) to right (B_3A_3) in Fig. 1, the optical phase delay $\phi_3(\rho)$ introduced by the second axicon lens and the air is[28]

$$\phi_3(\rho) = kn\delta_3 - kn_0 \frac{\rho^2}{2f}, \tag{10}$$

where δ_3 is the thickness of the focusing lens along its optical axis and f is the focal length of the focusing lens. So

Downloaded From: https://www.spiedigitallibrary.org/journals/Optical-Engineering on 27 Aug 2019
Terms of Use: https://www.spiedigitallibrary.org/terms-of-use

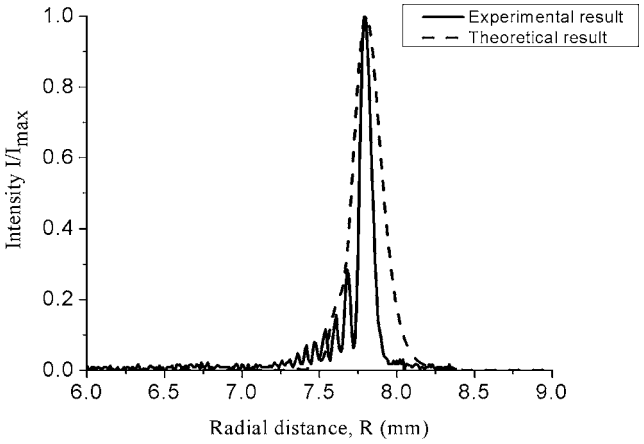

Fig. 3 A small part of the transverse cross section of a large annular beam, showing the radial variation of the irradiance profile after passing through the first axicon lens. Here $z'=71$ mm, $r_w=0.327$ mm.

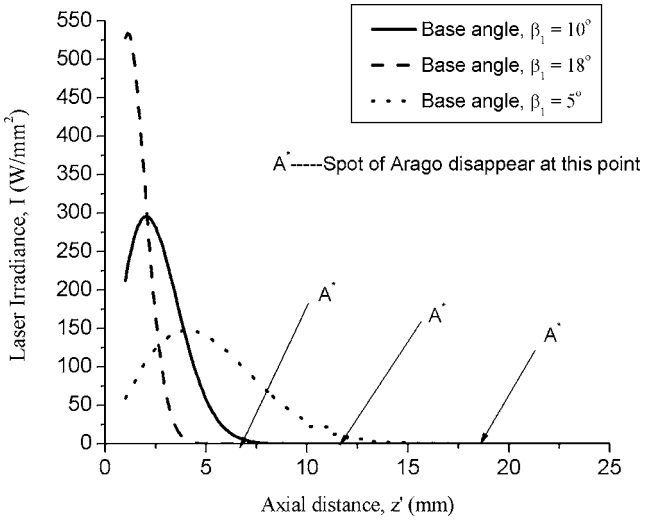

Fig. 4 Variations of the theoretical laser irradiance distributions $I(0,z)$ along the z axis ($r=0$) after the first axicon lens for different base angles, to check where the spot of Arago disappears (point A^* in this figure) so that the second axicon lens can be placed there. Here $r_w=0.327$ mm and $I_0=1$ W/mm^2.

the transmittance function $t_3(\rho)$ of the focusing lens is

$$t_3(\rho)=\begin{cases}\exp[i\phi_3(\rho)] & \text{for } \rho<\rho_1,\\ 0 & \text{for } \rho\geqslant\rho_1.\end{cases} \tag{11}$$

Neglecting the constant phase factor $\exp(ikn\delta_3)$,[29] the diffraction field, $U_3(\eta,L)$ at a distance L from the focusing tip O_3 along the optical axis can be written as follows in polar coordinates for rotationally symmetric systems by the Fresnel diffraction integral:[29]

$$U_3(\eta,L)=\frac{k\exp(ikL)}{iL}\exp\left(\frac{ik\eta^2}{2L}\right)\int_0^{\rho_1}U_2(\rho,Z')\times\exp\left(\frac{ik\rho^2}{2L}\right)\exp\left(\frac{-ik\rho^2}{2f}\right)J_0\left(\frac{k\rho\eta}{L}\right)\rho\,\mathrm{d}\rho. \tag{12}$$

3 Laser Irradiance Distributions at Different Locations of the Axicon Refractive System

3.1 *Laser Irradiance Distributions after the first Axicon Lens*

The laser irradiance profiles are calculated using the previously mentioned diffraction patterns. As shown in Fig. 1, an input Gaussian (TEM_{00}) Nd:YAG laser beam of wavelength $\lambda=1.064$ μm is incident on the flat surface of the first axicon lens with the beam axis lying on the principal axis of the axicon lens. The waist of the Gaussian beam was located inside the Nd:YAG laser cavity. A collimated horizontal beam from the exit of the laser system was turned to a vertical beam with a 45-deg mirror to direct it to the first axicon lens. Both axicon lenses and the focusing lens are made of fused silica of refractive index $n=1.46$. The half apex angles of the axicon lenses are $\alpha_1=\alpha_2=72$ deg, and their base angles are $\beta_1=\beta_2=18$ deg, as shown in Fig. 1. The focal length of the convex lens is $f=50$ mm. The incident beam profiles are shown in Fig. 2. The annular beam irradiance profiles were measured with a CCD camera (Laser Cam II, 4.7×5.5-μm pixel size). To obtain the diffraction patterns of the annular beam at different axial locations of the axicon lens system, the CCD camera was placed on a translation stage to adjust its position in the optical system.

Figure 3 shows the measured irradiance profile after the beam passes through the first axicon lens. Several rings are generated around the annular region, i.e., several low irradiance inner diffraction rings are formed near the main high-irradiance thin outer ring. Most of the laser energy is focused onto the outer main ring. The performance of this narrower annulus is actually beneficial for optical trepanning, since the width of the annular beam (i.e., the difference between the inner and outer annular beam radii) significantly influences the drilled hole quality. This effect has been found to be very important,[2] because a wider annular laser spot increases the growth of melt layer in the radial direction. A thinner recast layer, smaller taper, and higher drilling speed are obtained for a fixed outer radius of a given annular beam with smaller annular width, i.e., with larger inner radius of the annular beam.

The measured width of the main annular ring is smaller than that predicted by the Fresnel diffraction integral. The discrepancy between the experimental and theoretical results may be due to several reasons: the blunt tip of the axicon, the imperfect incoming Gaussian beam, and aberrations and imperfections of the optical elements. The phase shift due to optical elements is calculated in this study by considering the incident beam as a plane wave at the input plane of each optical element. This approximation is strictly applicable for the beam waist plane within the Rayleigh zone. Outside of this plane, the beam involves a quadratic phase function in the paraxial approach. Therefore, the existence of a quadratic phase could also be responsible for the discrepancy between the experimental and theoretical results.

Figure 4 shows the theoretical longitudinal irradiance distributions along the z axis for different base angles of the

Downloaded From: https://www.spiedigitallibrary.org/journals/Optical-Engineering on 27 Aug 2019
Terms of Use: https://www.spiedigitallibrary.org/terms-of-use

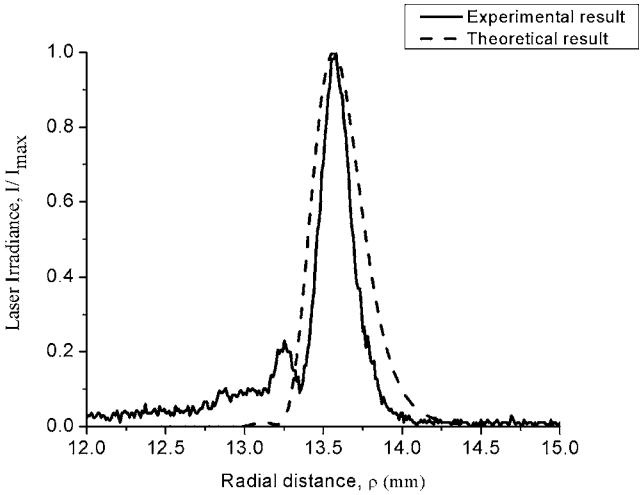

Fig. 5 A small section of a large annular beam, showing radial variation of the irradiance profile after passing through the second axicon lens. Here r_w=0.327 mm, z'=95 mm, and Z'=50 mm.

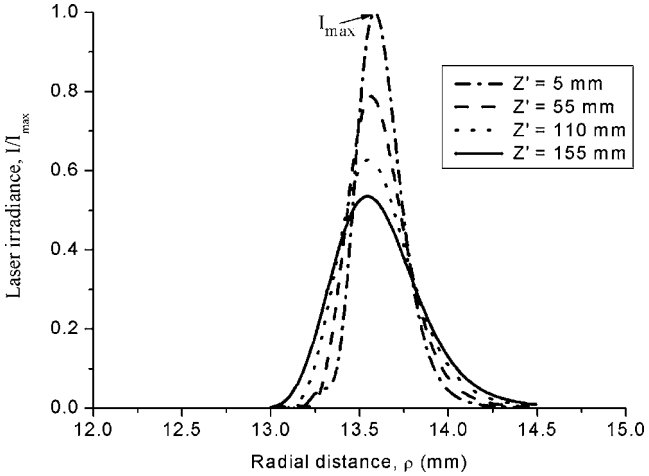

Fig. 6 Propagation of an annular beam after passing through the second axicon lens, showing the variation of the irradiance in the radial direction. Here r_w=0.327 mm, z'=95 mm, and Z'=110 mm.

axicon lenses. A spot with high irradiance is formed when the distance z' is less than 20 mm for the axicon lens with base angle β_1=5 deg. This is because most of the incident laser energy is focused into the optical axis of the axicon lens over a certain segment of the axis. Axicon lenses with small base angles have longer focus lines over which high irradiance spots are generated. To maximize the laser energy in the annular region, the second axicon lens should be placed after this region of focus during optical trepanning. Axicon lenses with large base angles should be chosen for a compact optical trepanning system.

It should be noted that the high-irradiance spots on the optical axis may be the spots of Arago.[26] The appearance of the bright line along the axis could also be due to the spherical aberration of the system. This bright spot is referred to as Arago's spot in this study, although, historically, Arago's spot is the one that appears in the geometrical shadow of an obstacle when light is diffracted by the obstacle.

3.2 *Laser Irradiance Distributions after the Second Axicon Lens*

Figure 5 shows the annular profile after the beam passes through the second axicon lens. As in the case of the first axicon lens, several inner diffraction rings and a main outer ring with maximum irradiance are found by the second axicon lens as well. The thickness of the main outer ring is much larger than that of the ring obtained after the first axicon lens. On the annular cross-sectional plane of the laser beam, both the experimental and theoretical irradiance profiles of the main ring are Gaussian-like (i.e., we have a Gaussian-like beam with maximum irradiance located at the center of the annulus).

Figure 6 shows the theoretical development of the annular beam after the second axicon lens. The width of the annulus increases and the maximum value of the irradiance decreases with the increase of the distance Z' between the first and the second axicon lenses. However, the radius of the center of the annulus remains almost the same as Z' increases from 5 to 155 mm, because of the collimation of the laser beam after the second axicon.

3.3 *Development of Imperfect Annular Beams and the Effect of the Focusing Lens on the Irradiance Profile*

The laser irradiance distributions after the focusing lens are investigated in this subsection. The blunt tip of an axicon lens produces an imperfect annular beam, i.e., an annulus with multiple diffraction rings, as illustrated in Fig. 7. Such rings are absent in the theoretical result because the model is based on a perfect axicon lens, i.e., an axicon lens with pointed vertices, resulting in a perfect annular beam. The imperfection of the annular beam, i.e., the presence of multiple rings in the annulus, generates Arago's spot over a certain axial length around the focal point although the theory predicts Arago's spot only on the focal plane, as sketched in Fig. 7. The imperfect annular beam, i.e., an annulus with multiple diffraction rings, reappears after the focal plane in the experimental results, whereas a perfect annular beam appears in the theoretical result because the incident beam on the focusing lens is a perfect annular beam. These three observations and the laser irradiance profiles before the focal plane, on the focal plane, and after the focal plane are analyzed in Figs. 8–10 respectively.

Figure 8(a) shows the annular profile after the beam passes through the focusing lens. Here again, Arago's spot appears after the focusing lens due to the diffraction effect, even when the incident collimated annular beam does not contain any energy on the axis of the beam. Several diffraction rings disappear downstream after being converged by the focusing lens, leaving only one main outer ring with maximum irradiance. Figure 8(b) and 8(c) show the laser irradiance profiles along both the longitudinal direction and the transverse plane of the annular beam. On the transverse plane, the irradiance profile is a Gaussian-like distribution. The outer radius R_0 of the annular beam is defined as the distance between the center of the annular beam and the point where the irradiance of the laser beam is $1/e^2$ of the

Downloaded From: https://www.spiedigitallibrary.org/journals/Optical-Engineering on 27 Aug 2019
Terms of Use: https://www.spiedigitallibrary.org/terms-of-use

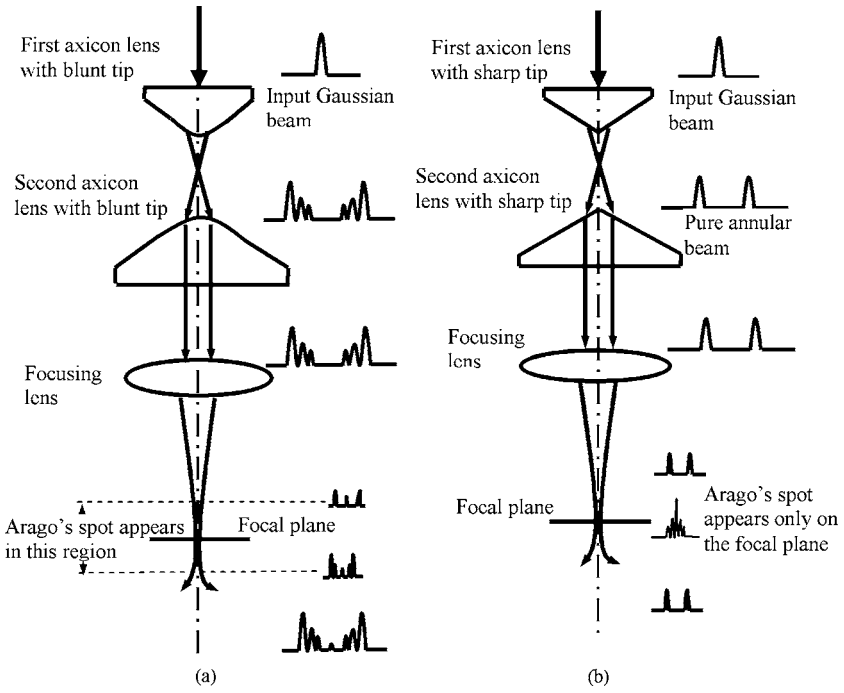

Fig. 7 Development of diffraction patterns the along axial direction in an annular beam shaped with a refractive axicon system. (a) Experimental diffraction patterns produced by an imperfect refractive axicon system. The imperfect axicon has a blunt vertex. (b) Theoretical diffraction patterns produced by a perfect refractive axicon system. The perfect axicon has a pointed vertex.

maximum irradiance I_0. A laser beam analyzer was used to plot the irradiance profile of the annular beam on a computer screen, where the irradiance point corresponding to $1/e^2$ of the maximum irradiance I_0 can be selected on the radial axis and the radius of this point can be determined using data acquisition software. The value of this radius is taken as the outer radius R_0.

Optical trepanning is expected to provide more flexibility in controlling the hole quality than traditional circular beam laser drilling, since an annular beam enables shaping of the laser irradiance profile to supply laser energy to the workpiece in a variety of ways. For percussion drilling, the irradiance profiles are usually either Gaussian or uniform. In optical trepanning, the geometry of the hole taper can be modified, viz., convergent or divergent holes can be produced using different types of irradiance profiles. Different profiles also can have important effects on the recast layer thickness, heat-affected zone (HAZ), and drilling speed. Figure 8 shows a Gaussian-like annular beam generated from an input Gaussian beam. Annular beams with various irradiance profiles can be obtained using axicon lenses with different curvatures of the conic surface.

It should be noted that the alignment of the optical elements is critical to obtain a good-quality annular beam. The elements must be illuminated at exactly normal incidence with coincident optical and laser-beam axes. Even a slightly oblique incidence will change the quality of the annular beam and effect the presence or disappearance of Arago's spot. The measured nonuniformly wide annular beam shown in Fig. 8 is mainly due to the imperfect alignment of the axicon lens system. Also, the incident laser beam must be perfectly circular to obtain a good-quality annular beam.

Experimental results show higher irradiance in Arago's spot and smaller beam radius than the corresponding theoretical results. This may be because the larger rings, which were considered in the theoretical calculation as the beam passes through the second axicon lens, do not affect the performance of the laser beam analyzer significantly, owing to the insensitivity of the instrument to the low energy content of the larger rings. The experimental annular ring was found to contain several narrow rings in the annulus before the focusing lens. When such multiple rings of the annulus are focused, some of them may be diffracted to the central spot. This creates Arago's spot with high irradiance in a region around the focal plane. According to the theoretical model, the annular beam before the focusing lens consists of a single wide ring. The focusing lens causes diffraction of this ring and produces Arago's spot only on the focal plane.

Figure 9 shows the theoretical diffraction pattern at the focal plane for an annular beam. The annular ring disappears, and a bright circular spot with very high irradiance appears at the laser beam center. In experiments, however, multiple diffraction rings are produced in the annulus after the second axicon lens, for the reasons mentioned earlier. These rings disappear after being converged by the focusing lens. Several diffraction rings, however, reappear after the focal plane, due to the divergence of the beam, as shown in Fig. 10.

3.4 *Effect of Focal Length on the Beam Radius*

Figure 11(a) and 11(b) show the variation of the outer radius of the annular beam with distance L between the fo-

Downloaded From: https://www.spiedigitallibrary.org/journals/Optical-Engineering on 27 Aug 2019
Terms of Use: https://www.spiedigitallibrary.org/terms-of-use

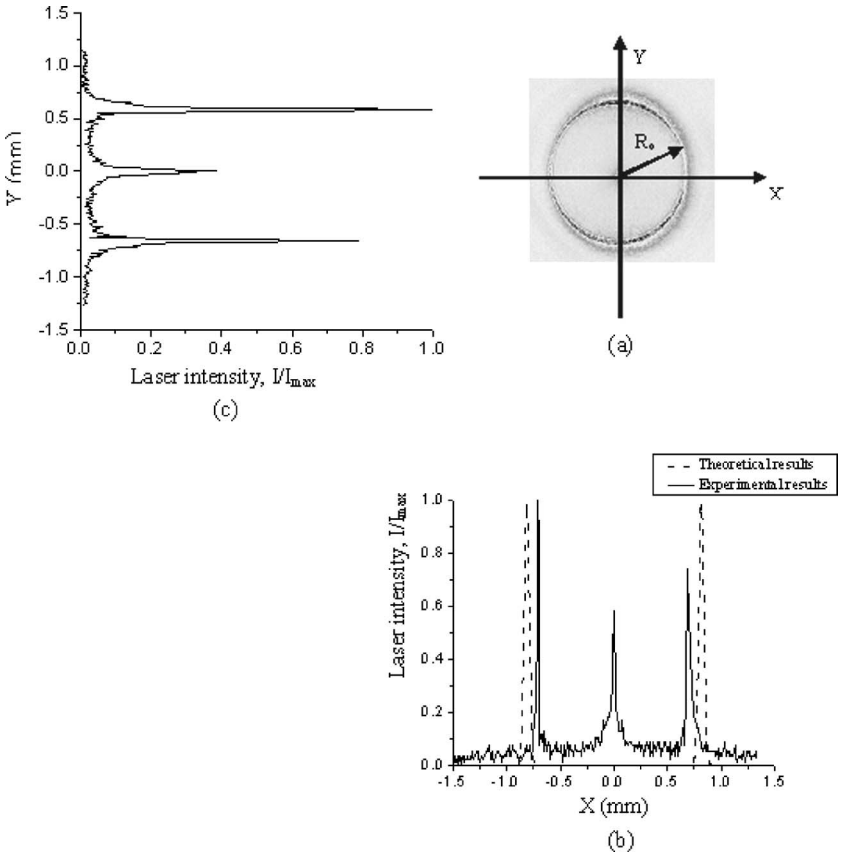

Fig. 8 Irradiance distributions of an annular beam before the focal plane at $L=47$ mm for a convex lens of focal length $f=50$ mm. (a) Transverse cross section of the annular beam profile. (b) Beam profile in the X direction on the transverse plane. (c) Beam profile in the Y direction on the transverse plane. Here $R_0=0.665$ mm, $r_w=0.327$ mm, $z'=95$ mm, and $Z'=110$ mm.

cusing lens and the observation plane. Annular beams of different diameters are obtained by adjusting L. For example, the outer radius of the annular beam is $R_0=1.02$ mm for $L=46$ mm, and $R_0=85$ μm for $L=49$ mm.

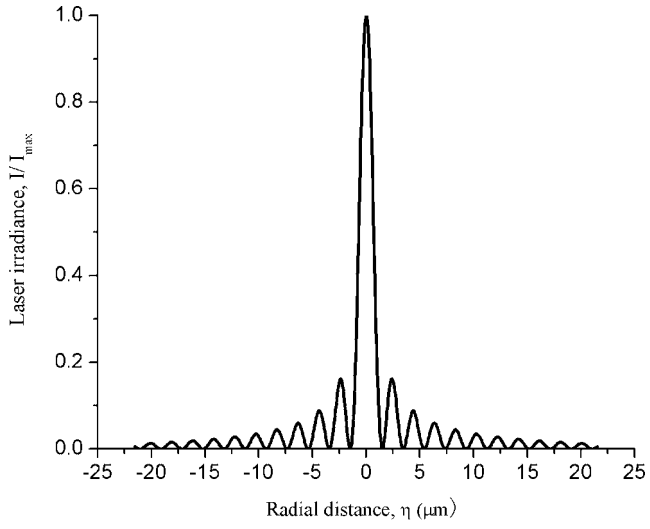

Fig. 9 Irradiance distributions along the radial direction at the focal plane. Here $f=50$ mm, $r_w=0.327$ mm, $z'=95$ mm, and $Z'=110$ mm.

The importance of this capability is that it provides tremendous flexibility to trepan holes having outer-radius variations over an order of magnitude, using a single optical system. Since the outer radius is a very sensitive function of L, this capability also enables drilling tapered holes by systematically varying L using a servo system during the drilling process.

Fig. 11(a) shows that the theoretical and experimental values of R_0 do not match for the nominal focal length $f=50$ mm. The discrepancy could be due to the manufacturing tolerance in the focal length of the convex lens. This type of focal shift is also observed in diffracted converging spherical waves,[27] where the focal shift due to this effect is given by $\Delta f=-f/(1+\pi^2N^2)$ and $N=a^2/\lambda f$ for a Gaussian beam. We have $\Delta f=1.337$ μm for the typical case with $a=14.2$ mm, $\lambda=1.064$ μm, and $f=50$ mm in this study. On the other hand, the specification on the focal length of the focusing lens was 50 mm$\pm$2% due to the manufacturing tolerance. So theoretical calculations were carried out to determine the annular beam radius R_0 for different values of the focal length f. The values of R_0 were found to be closer to the experimental results for $f=49.3$ than for $f=49.5$ and 50 mm. The remaining discrepancy between the experimental and theoretical results may be due to spherical aberration, which is the most important of all primary aberrations, caused by different focal positions for marginal

Downloaded From: https://www.spiedigitallibrary.org/journals/Optical-Engineering on 27 Aug 2019
Terms of Use: https://www.spiedigitallibrary.org/terms-of-use

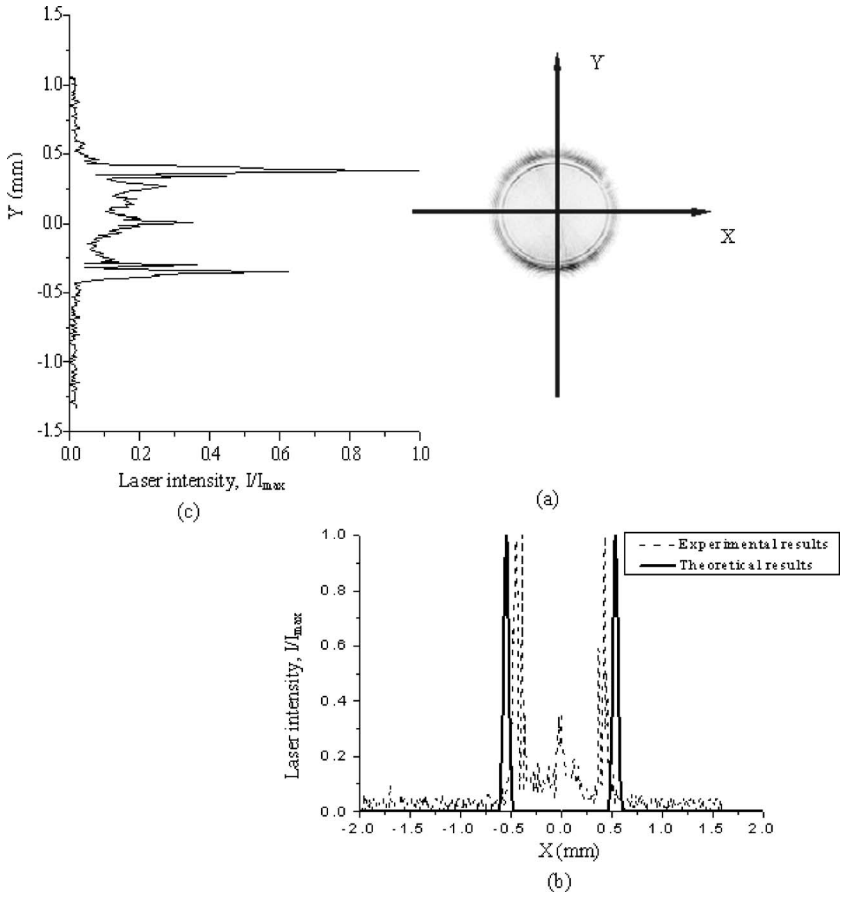

Fig. 10 Irradiance distributions of the annular beam at 2 mm after the focal plane (i.e., at $L=52$ mm). (a) Transverse cross section of the annular beam profile. (b) Beam profile in the X direction on the transverse plane. (c) Beam profile in the Y direction on the transverse plane. Here $f=50$ mm, $L=52$ mm, $r_w=0.327$ mm, $z'=95$ mm, and $Z'=110$ mm.

meridional and paraxial rays. For lenses with spherical surfaces, the rays that are parallel to the optical axis but at different distances from it fail to converge to the same point after passing through the lens. This effect changes the annular profiles and the corresponding diffraction patterns. According to the theoretical model, the minimum diameter of the annular beam is $R_0=90$ μm for an axicon system with $r_w=0.327$ mm, $z'=95$ mm, $Z'=110$ mm, and $f=49.3$ mm. This value of R_0 is very close to the experimental radius of 85 μm [Fig. 11(b)].

Smaller-radius annular beams can be achieved with lasers having shorter wavelengths. Increasing the diameter of the input laser beam or decreasing the focal length of the focusing lens can also decrease the radius. Finally, the radius decreases as the plane of observation approaches the focal plane of the focusing lens. However, more and more laser energy accumulates on the optical axis near the focal plane, which limits the minimum beam size.

4 Conclusions

An axicon refractive system has been designed to convert an input Gaussian beam into an annular beam. The diffraction patterns generated by different optical elements of the system are investigated by using the Fresnel diffraction integral. The laser irradiance profiles produced by the system were measured using a laser-beam analyzer. The following conclusions can be drawn, based on the numerical solutions and measured annular profiles:

1. A Gaussian-like annular beam can be produced with an axicon refractive system. The beam diameter decreases as the plane of observation approaches the focal plane of the focusing lens. However, the minimum beam diameter is limited by the diffraction effect.
2. A thin outer annulus with maximum irradiance and several inner diffraction rings with lesser irradiance were found to form due to diffraction.
3. More and more laser energy accumulates on the optical axis of the axicon lens system over a small region around the focal plane. The annular ring disappears at the focal plane and reappears after the focal plane.
4. The optical elements need to be aligned to generate radially symmetric irradiance profiles, which is important for drilling circular holes. Optical trepanning can be applied to drill small holes with low-power lasers, since relatively high irradiance can be obtained with a small area of the annular beam. A large area of the annular beam reduces the irradiance for a

Downloaded From: https://www.spiedigitallibrary.org/journals/Optical-Engineering on 27 Aug 2019
Terms of Use: https://www.spiedigitallibrary.org/terms-of-use

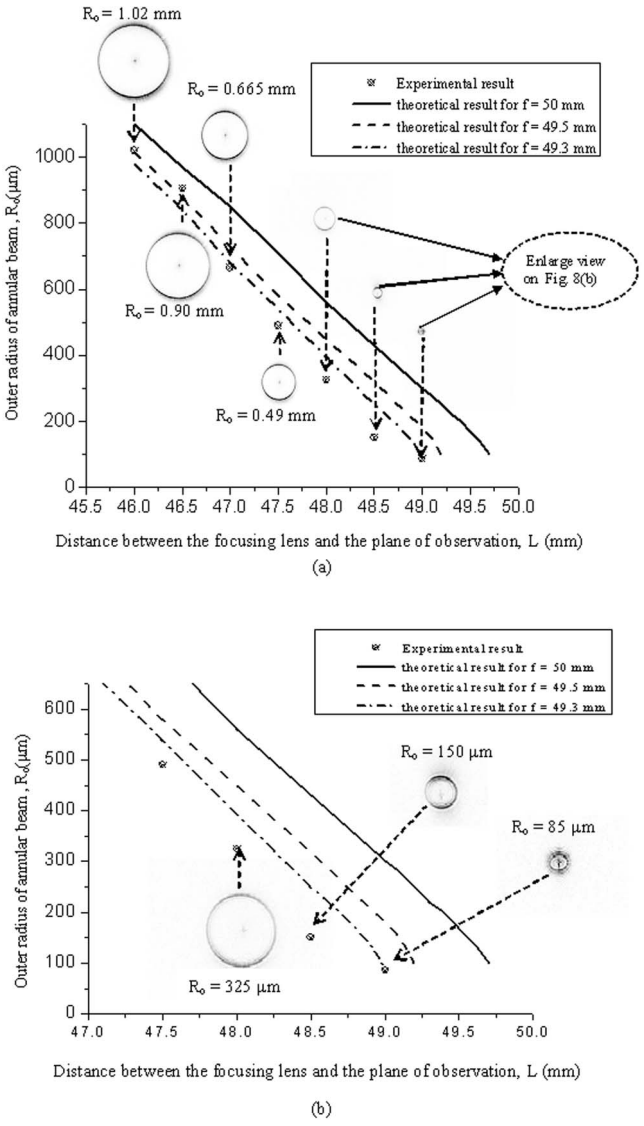

Fig. 11 Outer diameter of an annular beam at different axial locations after passing through a convex lens. Here r_w=0.327 mm, z' =95 mm, Z'=110 mm, and f=50, 49.5, and 45.3 mm. The lower right part of (a) is shown enlarged in (b).

given laser power. Therefore, high-power lasers would be necessary for optical trepanning of large holes in thick samples.

Acknowledgments

This research was supported by Laser Fare, Inc., Smithfield, RI, under a USAF/MDO SBIR Phase II project on laser drilling under contract F29601-03-C-0192 to the U.S. Air Force Research Laboratory, Albuquerque, NM. Dr. W. P. Latham is the program manager who originally proposed the optical trepanning concept. Dr. P.F. Jacobs is the principal investigator of the project at Laser Fare, Inc.

References

1. J. F. Ready and D. F. Farson, "Components for laser materials processing systems," Chap. 4 in *LIA Handbook of Laser Material Processing*, pp. 134–139, Magnolia Publishing, Orlando, FL (2001).
2. D. Zeng, W. P. Latham, and A. Kar, "Two-dimensional model for melting and vaporization during optical trepanning," *J. Appl. Phys.* **97** (in press).
3. I. Manek, Y. B. Ovchinnikov, and R. Grimm, "Generation of a hollow laser beam for atom trapping using an axicon," *Opt. Commun.* **147**, 67–70 (1998).
4. J. E. Molloy and M. J. Padgett, "Lights, action: optical tweezers," *Contemp. Phys.* **43**, 241–158 (2002).
5. S. Kulin, S. Aubin, S. Christe, B. Peker, S. L. Rolston, and L. A. Prozco, "A single hollow-beam optical trap for cold atoms," *J. Opt. B: Quantum Semiclassical Opt.* **3**, 353–357 (2001).
6. H. J. Metcalf and P. V. Straten, "Laser cooling and trapping of atoms," *J. Opt. Soc. Am. B* **20**, 887–908 (2003).
7. M. Rioux, R. Tremblay, and P. A. Belanger, "Linear, annular, and radial focusing with axicons and applications to laser machining," *Appl. Opt.* **17**, 1532–1536 (1978).
8. P. A. Belanger and M. Rioux, "Ring pattern of a lens-axicon doublet illuminated by a Gaussian beam," *Appl. Opt.* **17**, 1080–1086 (1978).
9. M. R. Descour, D. I. Simon, and W. H. Yeh, "Ring-toric lens for focus-error sensing in optical data storage," *Appl. Opt.* **38**, 1388–1392 (1999).
10. J. H. Mcleod, "The axicon: a new type of optical element," *J. Opt. Soc. Am.* **44**, 592–597 (1954).
11. Z. Jaroszewicz, A. Burvall, and A. T. Friberg, "Axicon—the most important optical element," *Opt. Photonics News* **16** 34–38, (2005).
12. J. Lloyd, K. Wang, A. Barkan, and D. M. Mittleman, "Characterization of apparent superluminal effects in the focus of an axicon lens using terahertz time-domain spectroscopy," *Opt. Commun.* **219**, 289–294 (2003).
13. Y. Song, D. Milam, and W. T. Hill III, "Long, narrow all-light atom guide," *Opt. Lett.* **254**, 1805–1807 (1999).
14. M. de Angelis, L. Cacciapuoti, G. Pierattini, and G. M. Tino, "Axially symmetric hollow beams using refractive conical lenses," *Opt. Lasers Eng.* **39**, 283–291 (2003).
15. J. R. Flores, "General method to design spherically symmetric GRIN axicons," *J. Mod. Opt.* **48**, 493–506 (2001).
16. A. Thaning and A. T. Friberg, "Design of diffractive axicons producing uniform line images in Gaussian Schell-model illumination," *J. Opt. Soc. Am. A* **19**, 491–495 (2002).
17. J. Sochacki, A. Kolodzjejczyk, Z. Jaroszewicz, and S. Bara, "Nonparaxial design of generalized axicons," *Appl. Opt.* **31**, 5326–5330 (1992).
18. A. Thaning, Z. Jaroszewicz, and A. T. Friberg, "Diffractive axicons in oblique illumination: analysis and experiments and comparison with elliptical axicons," *Appl. Opt.* **42**, 9–17 (2003).
19. S. Y. Popov and A. T. Friberg, "Design of diffractive axicons for partially coherent light," *Opt. Lett.* **23**, 1639–1641 (1998).
20. Z. Jaroszewich and J. Morales, "Lens axicons: systems composed of a diverging aberrated lens and a converging aberrated lens," *J. Opt. Soc. Am. A* **16**, 191–197 (1999).
21. V. Garces-Chavez, D. McGloin, H. Melville, W. Sibbett, and K. Dholakia, "Simultaneous micromanipulation in multiple planes using a self-reconstructing light beam," *Nature (London)* **419**, 145–147 (2002).
22. R. M. Herman and T. A. Wiggins, "Production and uses of diffractionless beams," *J. Opt. Soc. Am. A* **8**, 932–942 (1991).
23. J. Durnin, "Exact solutions for nondiffracting beams. I. The scalar theory," *J. Opt. Soc. Am. A* **4**, 651–654 (1987).
24. J. Durnin, J. J. Meceli, and J. H. Eberly, "Diffraction-free beams," *Phys. Rev. Lett.* **58**, 1499–1501 (1987).
25. D. Malacara and Z. Malacara, "Spherical aberration," Chap. 5 in *Handbook of Lens Design*, pp. 123–129, Marcel Dekker, Inc., New York (1994).
26. J. E. Harvey and J. L. Forgham, "The spot of Arago: new relevance for an old phenomenon," *Am. J. Phys.* **52**, 243–247 (1984).
27. Y. Li and E. Wolf, "Focal shifts in diffracted converging spherical waves," *Opt. Commun.* **39**, 211–215 (1981).
28. M. V. Perez, C. Gomez-Reino, and J. M. Cuadrado, "Diffraction patterns and zone plate produced by thin linear axicons," *Opt. Acta* **33**, 1161–1176 (1986).
29. J. W. Goodman, "Fresnel and Fraunhofer diffraction," Chap. 4 in *Introduction to Fourier Optics*, J. W. Goodmen, Ed., pp. 66–73, McGraw-Hill, Inc., Singapore (1996).

D. Zeng received his master's degree from the Jiangsu University in China. He is a graduate student of optics and MMAE at UCF. His research interests are in the areas of laser-aided manufacturing, materials, and microprocessing.

Downloaded From: https://www.spiedigitallibrary.org/journals/Optical-Engineering on 27 Aug 2019
Terms of Use: https://www.spiedigitallibrary.org/terms-of-use

W. P. Latham is chief of the Cooperative Development Branch at the Air Force Research Laboratory, Directed Energy Directorate, Kirtland Air Force Base, New Mexico. His primary research areas have been laser theory, including optical resonator theory and optical physics, and light scattering theory, including laser-beam–material interaction. He has analyzed and designed several novel resonant cavities for use with high-power lasers. He has worked to transfer government-developed laser technology to the commercial sector. This effort has led to an increasing involvement with applications of lasers, including medical applications and laser materials processing research.

A. Kar received his PhD degree from the University of Illinois at Urbana-Champaign and is an associate professor of optics, MMAE, and physics at UCF. His research interests are in the areas of laser-aided manufacturing, materials, and microprocessing.

Downloaded From: https://www.spiedigitallibrary.org/journals/Optical-Engineering on 27 Aug 2019
Terms of Use: https://www.spiedigitallibrary.org/terms-of-use